Available online at www.sciencedirect.com
SCIENCE DIRECT®
Journal of Molecular Catalysis A: Chemical 239 (2005) 1–9
JOURNAL OF MOLECULAR CATALYSIS A: CHEMICAL
www.elsevier.com/locate/molcata

Iron(III)protoporphyrin/MCM41 catalyst as a peroxidase enzyme model: Preparation and typical test reactions

K. Nazari [a,b,*], S. Shokrollahzadeh [a], A. Mahmoudi [c], F. Mesbahi [b], N. Seyed Matin [b], A.A. Moosavi-Movahedi [d,e]

[a] *Chemistry Dept., Shahr-Rey Islamic Azad University (IAU), P.O. Box 18735/334 Tehran, Iran*
[b] *Research Institute of Petroleum Industry, N.I.O.C., P.O. Box 18745/4163 Tehran, Iran*
[c] *Chemistry Department, Karaj Islamic Azad University, Karaj, Iran*
[d] *Institute of Biochemistry and Biophysics, University of Tehran, Tehran, Iran*
[e] *Center of Excellence for Interdisciplinary Sciences, IAU, Tehran, Iran*

Received 9 January 2005; received in revised form 4 May 2005; accepted 5 May 2005
Available online 5 July 2005

Abstract

MCM41 was synthesized and Fe(III)protoporphyrin(IX) (Hemin, Fe(III)PPIX) was directly encapsulated into MCM41 pores through the self-assembly formation mechanism using micelles of quaternary alkylammonium salt (cetyl trimethyl ammonium bromide) as the solvent for Fe(III)PPIX and template for formation of MCM41 spontaneously. The catalysts obtained were characterized by XRD, BET N_2 adsorption isotherm, diffuse reflectance UV–vis and FT-IR techniques. Fe(III)PPIX/MCM41 was used in some typical test reactions, such as oxidation of phenol, *ortho*-methoxyphenol (guaiacol) and synthesis of indophenol. Kinetic parameters including initial reaction rates, rate constants, V_{max}, turnover number, Michaelis constant and catalytic efficiency were obtained and compared to those of Fe(III)/MCM41(as a blank) and horseradish peroxidase (HRP) enzyme (consisting of Fe(III)PPIX as the prosthetic group). Results showed that Fe(III)PPIX/MCM41 catalyst was able to mimic horseradish peroxidase with a K_m value of 183 μM with respect to guaiacol (as the reducing substrate of HRP). Fe(III)PPIX/MCM41 catalyzes the oxidation reactions (in the presence of hydrogen peroxide) at higher rates than the homogeneous Fe(III)PPIX system and Fe(III)/MCM41 heterogeneous catalyst, but at lower rates than the enzyme as a homogeneous catalytic system.

Keywords: MCM41; Iron(III)protoporphyrin; Heme encapsulation; Peroxidase; Oxidation

1. Introduction

In contrast to heterogeneous catalysts, homogeneous ones have disadvantages, such as lower stability and less successful separation from the reaction mixture. Despite their higher activity, metalloporphyrins are capable of catalyzing some reactions, such as oxidation, epoxidation and hydroxylation of organic compounds [1–5]. Fe(III)protoporphyrin(IX) (PPIX) may be found as a common catalytic active site in hemoproteins like hemoglobin, myoglobin, cytochromes and peroxidases[6,7]. This slightly water soluble catalyst can decompose hydrogen peroxide through a two-electron oxidation–reduction mechanism [8]. Iron porphyrins are biocatalysts, which catalyze oxidative reactions by decomposing hydrogen peroxide at the expense of various substrates, such as phenols and amides [9]. There is great interest in metalloporphyrins for analytical, synthetic and biotechnological purposes. Metalloporphyrins have low stability in water solutions so that they may become inactivated at extreme conditions (severe acidic or alkaline pHs, high temperatures, high concentrations of peroxide (>2 mM) and in the presence of reactive solvents) [8]. Furthermore, the catalytic activity of these catalysts in aqueous solutions may decrease by dimerization of heme molecules due to the low reactivity of dimeric ferriheme toward hydrogen peroxide [2,4]. The

* Corresponding author. Tel.: +98 21 4409471; fax: +98 21 4409471.
E-mail address: nazarikh@ripi.ir (K. Nazari).

1381-1169/$ – see front matter © 2005 Elsevier B.V. All rights reserved.
doi:10.1016/j.molcata.2005.05.010

stability of a biocatalyst during synthesis/purification processes and in operational conditions is of vital importance in biotechnology. Several strategies are at hand to increase operational stability of a biocatalyst including the use of stabilizing additives, immobilization, encapsulation, crystallization and medium engineering. Impregnation and encapsulation of these catalysts into pores of mesoporous molecular sieves lead to protection, stabilization and activation of these catalysts [10–15].

In 1992, a novel family of mesoporous silicate-based materials, the M41S materials, was invented by the researchers at Mobil company [16–19]. There is a great deal of interest in this family of mesoporous materials, which exhibit highly uniform mesoporous structures [16,17]. Given their ordered channel systems, uniform apertures in the range of 2–10 nm diameter and surface areas of greater than 900 $m^2\,g^{-1}$, the M41S materials, have expanded the pore size related applications of zeolite-like molecular sieves from the microporous regime. Since the pores in these mesoporous molecular sieves are accessible to bulky reactants, the encapsulating of nanometer size guest compounds or clusters become possible now. Furthermore, the reactive hydroxyl groups on the internal surface of these mesoporous hosts could be easily modified by covalently anchoring organometallic complexes or grafted by silane coupling agents [20–30]. Typical procedures for impregnation of metal complexes, such as metalloporphyrin and phthalocyanines, into mesopores of MCM have been previously reported [31–39].

In the present work encapsulation of a biocatalyst, iron(III)protoporphyrin and preparation of a heterogeneous enzyme model catalyst via direct synthesis of iron(III)-protoporphyrin/MCM41 is reported as well as its capability for mimicking the peroxidase enzyme reactions.

2. Experimental

2.1. Materials

Protoporphyrin(IX), Fe(III)PPIX and CTAB were obtained from Sigma. Sodium silicate solution (27%), tetramethylammonium hydroxide (TMAOH), hydrogen peroxide, phenol, guaiacol and iron(III) nitrate were purchased from Merck and used without further purification. All solutions were prepared using deionized water (Barstead NanoPure D4742; E.R. = 18 MΩ).

The obtained molecular sieve was characterized by X-ray diffraction using a Seifert diffractometer model 3003 using Cu Kα radiation. BET isotherms are obtained based on N_2 adsorption experiments using a Micromeritics ASAP 2010 instrument. Furthermore, diffuse reflectance UV–vis and IR (KBr wafer method) techniques were used for comparative investigation of various prepared catalysts using Cary 500 Varian and Bomem 100 spectrophotometers, respectively.

3. Methods

3.1. Synthesis of MCM41

The direct synthesis of MCM41 based catalysts followed a two-stage mechanism in which surfactant micelles were first self-assembled at the substrate–liquid interface. Inorganic silicates were then adsorbed and condensed on the micelles, forming an inorganic–organic nanocomposite [40–42]. The film formation was considered to involve the polymerization of silicate species in the aqueous solution and at the head region of the surfactant micelles [43]. The silica-surfactant self-assembly process occurs both at the solid–liquid and the liquid–vapor interfaces. Various reports on the synthesis and application of MCM materials are found in the literature [44–51].

MCM41 was synthesized by dispersion of sodium silicate (2.500 g) in deionized water (18.24 mL deionized water, molar ratio H_2O/silicalite = 45). After stirring the components, the surfactant cetyltrimethylammonium bromide (CTAB, 2.170 g) was added. The reaction mixture was stirred for 45 min at room temperature. During the vigorous stirring, an adequate amount of a 25% solution of tetramethyl ammonium hydroxide was added and the pH was adjusted at 10.5–11.0. The mixture was stirred at room temperature for 24 h, and then introduced into a teflon-lined autoclave and kept in it at 100 °C for 3 days. The powder was recovered by filtration, and subsequently washed with acidic water–ethanol solution. It was dried in a vacuum oven and the obtained solid was calcined at 500 °C for 4 h.

3.2. N_2 adsorption experiment

The previously adsorbed gases and vapors were removed from MCM41 as much as possible. For this purpose, a reduced pressure of 10^{-4} Torr (out gassing) was applied for 10 h. The volumetric method was used for determining the specific surface area and the average pore size of MCM41. The adsorbate, which was used for BET surface area determination, was nitrogen at 77 K.

The adsorption isotherm is obtained from a series of measurements at different pressures using a Micromeritics ASAP 2010 instrument. The BET model was also applied to evaluate the adsorption parameters of porous solid MCM41 [52–55].

3.3. Preparation of catalysts

Fe^{3+}MCM41 was prepared based on the Petridis method [56]. For this purpose Fe^{3+} (5.0 mg $Fe(NO_3)_3$/20.0 mg MCM41) was impregnated into MCM41. Fe(III)PPIX/MCM41 was prepared by direct encapsulation of an alkaline solution of hemin chloride (0.020 g, Fe(III)PPIX chloride) into the pores via the CTAB micelles, and after crystallization, filtration and efficient washing of the powder, the obtained catalyst was dried in a vacuum oven at 150 °C for 1 h. The amount of hemin encapsulated

in MCM41 was determined by measuring the iron content of the digested sample in a caustic solution using atomic absorption spectroscopy and was equal to 0.07% (w/w).

Furthermore, an indirect method of impregnation of Fe(III)PPIX into pure MCM41 was examined in which a 1 mM hemin solution was stirred with 1 g calcined MCM41 at 27 °C for 3 days and the obtained catalyst dried as described above. Experiments revealed that impregnation was not successful and the obtained catalyst did not have considerable catalytic activity.

3.4. Kinetic analysis

Kinetic studies on the catalytic oxidation of phenolic compounds in the presence of hydrogen peroxide were followed using a double beam Shimadzu spectrophotometer model 2101 PC. Steady-state kinetics of guaiacol (as a hydrogen donor) oxidation by hydrogen peroxide catalyzed by enzyme model (iron(III)protoporphyrin/MCM41) catalyst was obtained at 470 nm (colored product of the reaction) [57] in 2.5 mM phosphate buffer, pH 7.0. Progress curves of reactions were obtained at various guaiacol concentrations and the obtained initial rates used to record the Michaelis–Menten curves. The concentration of H_2O_2 was kept high and constant with respect to hydrogen donor (AH) during the course of reaction to ensure pseudo-first order kinetics. In a period of 120 s during which the progress curves were recorded, specified amounts of catalyst (10.0 mg), guaiacol (0.2–10 mM in the vessel) and hydrogen peroxide (0.25 mM in the vessel) were added, respectively, to a 30 mL temperature controlled vessel and initial rate of reaction (υ_i) was calculated from time domain of 45 s at the linear portion of the curve. In order to reach the steady-state condition, a lag time of 7 s was used. H_2O_2 stock solutions were prepared by appropriate dilutions of 30% (v/v) H_2O_2 in deionized water. The concentrations of hydrogen peroxide were determined by absorbance measurements at 240 nm using ε_{240} as 43.6 cm^{-1} M^{-1} [58] and the dilute solutions were freshly prepared.

Furthermore, another typical reaction, such as conversion of phenol to indophenol, was used for evaluation of capability of the catalyst to mimic the catalytic behavior of HRP. Progress curves for conversion of phenol to indophenol were obtained in the presence of 0.020 g Fe(III)PPIX/MCM41 catalyst. Details of experimental conditions are shown in the legends of figures.

4. Results and discussion

The surfactant/silica molar ratio in the synthesis mixture has been reported to be a critical variable in the formation of liquid-crystal template M41S materials [43]. At the molar ratio of surfactant/silica = 0.05, MCM41 (hexagonal phase) was obtained regardless of the sodium ion content.

pH dependency of the MCM formation as a function of time is shown in Fig. 1. The figure represents a minimum

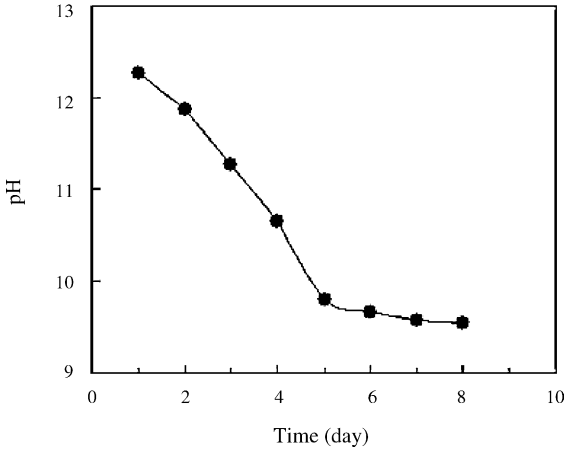

Fig. 1. pH of the reaction mixture for synthesis of MCM41 as a function of time.

time of 5 days for completion of crystallization process. Fig. 2 shows the XRD pattern of the synthesized and calcined MCM41, which exhibits a strong [1 0 0] reflection peak with two small peaks, characteristic of MCM41 mesoporous material [59–61].

Fig. 3 represents the BET plot for N_2 adsorption on MCM41 at 77 K. MCM41 consists mostly of long-range ordered hexagonal arrays of uniform mesopores [62,63]. The peak at [1 0 0] in X-ray diffractional spectra provides an independent estimate of the pore size in MCM41. The conventional method of determining pore size is the nitrogen adsorption method [64]. Usually nitrogen adsorption–desorption isotherms of MCM41 exhibit a sharp step commencing at $p/p_o = 0.3$, as shown in Fig. 3, and the reversible type IV isotherms without hysteresis [15]. The inflection point is attributed to the commencement of pore filling from which the pore diameter can be roughly estimated.

In addition, a number of theories have been developed for deriving parameters of pore structure from such a method; the applicability and accuracy for estimating the pore struc-

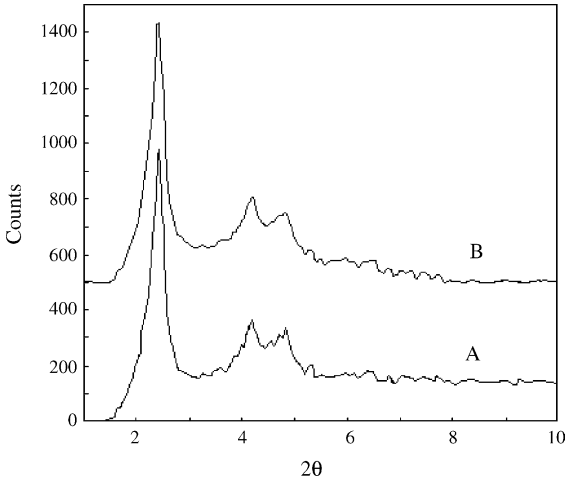

Fig. 2. X-ray diffraction pattern of calcined MCM41.

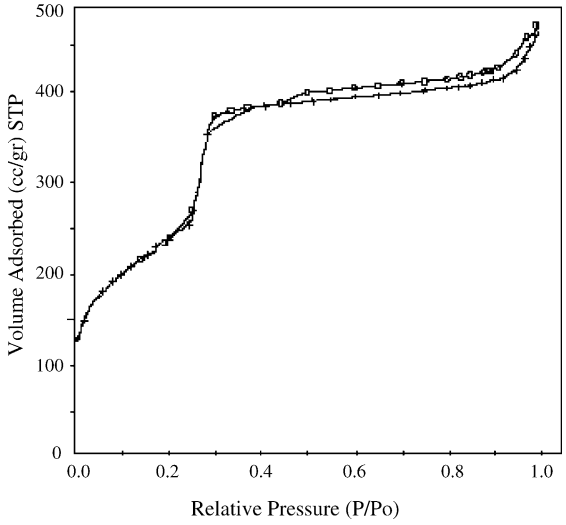

Fig. 3. Isotherms for multilayer adsorption and desorption of N_2 on MCM41 at 77 K: (+) adsorption and (o) desorption.

ture of solids, which consist of supermicropores and small mesopores are often in question [65]. Recently, a comprehensive comparison of different methods (NLDFT method, hydraulic radius approach and the geometric method based on the ideal model) for evaluating the pore size of MCM41 using nitrogen, neopentane, *n*-hexane, benzene and methanol adsorption isotherms has been reported [66]. The main feature of this study is the remarkable agreement and good results obtained from NLDFT and geometric methods. An average density value of 0.84 g cm^{-3} is suggested for estimating the liquid volume and the surface area is calculated using a value of 0.131 nm^2 for the cross sectional area instead of normally used value (0.162 nm^2). According to Fig. 3, a good reversibility is observed on adsorption and desorption processes and an average pore size is obtained about 3.7 Å associated with a sharp distribution pore size around this point.

Fig. 4(a and b) show the diffuse reflectance UV–vis electronic spectra for the MCM41 and Fe(III)PPIX/MCM41 catalysts in which the impregnation and substitution of Fe(III)PPIX into the mesopores is indicated [67]. Peroxidase enzyme has a sharp Soret band absorption spectra at 403 nm, while such an absorption was observed as a broad band at 360–390 nm for Fe(III)PPIX solution. As Fig. 4(b) shows Fe(III)PPIX/MCM41 indicates a similar absorption band at 403 nm, quite similar to that of the peroxidase enzyme. Fig. 5(a and b) show typical FT-IR spectra of the MCM41 and Fe(III)PPIX/MCM41 samples. Characteristic absorption peaks confirm the MCM41 structure [68–72].

4.1. Chemical catalysis

Fig. 6 shows the catalytic activity of the Fe(III)-PPIX/MCM41 for the oxidation of guaiacol as described in Section 3.4. Steady-state kinetics of guaiacol oxida-

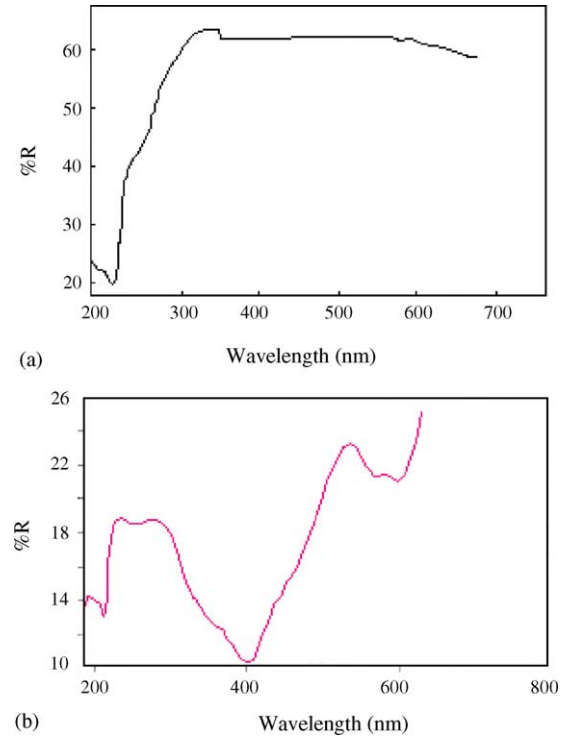

Fig. 4. Diffuse reflectance UV–vis spectra of catalysts: (a) MCM41 and (b) Fe(III)PPIX/MCM41.

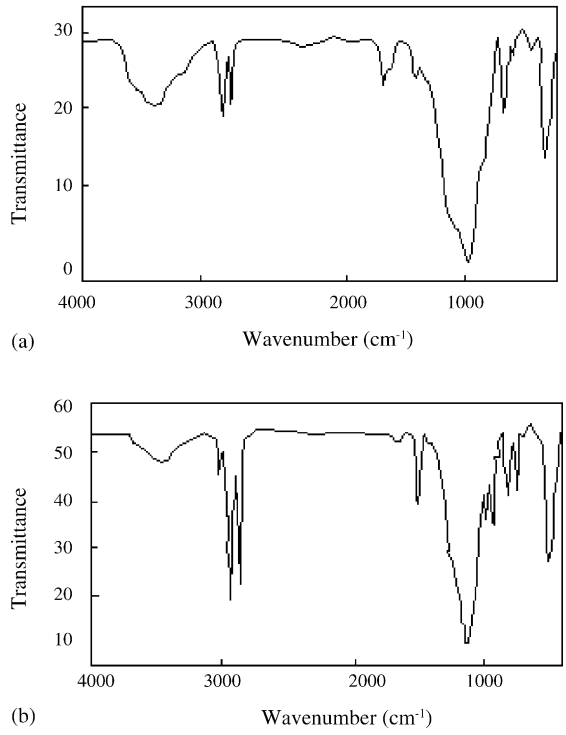

Fig. 5. FT-IR spectra of catalysts in KBr wafer resolution = 4 cm^{-1}, scan rate = 21 scans min^{-1} and number of scans = 12; (a) MCM41 and (b) Fe(III)PPIX/MCM41.

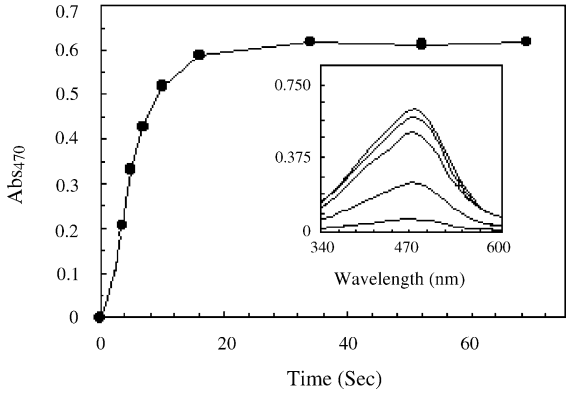

Fig. 6. Typical progress curve for oxidation of guaiacol by Fe(III)PPIX/MCM41, [guaiacol] = 2.8 mM, [H_2O_2] = 2.0 mM and Fe(III)PPIX/MCM41 = 0.010 g.

tion by hydrogen peroxide catalyzed by iron(III)protoporphyrin/MCM41 was carried out at 470 nm (colored product of the reaction) [57] in 2.5 mM phosphate buffer, pH 7.0. Progress curves of reactions were obtained at various guaiacol concentrations and the obtained initial rates were used to sketch the Michaelis–Menten curves. Fig. 6 inset shows the recorded overlaying spectra for progress of the reaction at 2 min intervals. Furthermore, Fig. 6 shows the corresponding progress curve for this oxidation as the absorbance of the colored product (tetraguiacol, λ_{max} = 470 nm) versus time. As the figure shows, the reaction is over within about 20 s.

Kinetic mechanism of the peroxidase enzyme reaction is well established [73]. The catalytic cycle involves distribution of the enzyme in forms of HRP (free enzyme), and active species **C_I** (compound I) and **C_{II}** (compound II). The oxidation–reduction reaction is associated with accumulation of free radicals of the aromatic compound (**$A^\bullet$**). Then, the polymerization step may occur via combining these active free radicals. A brief scheme of the peroxidase catalytic reaction cycle may be indicated as follows

$$\text{HRP} + H_2O_2 \rightarrow \text{Compound-I(HRP-Fe=O)} + H_2O$$

$$\text{Compound-I(HRP-Fe=O)} + \text{AH} \rightarrow \text{Compound-II(HRP-Fe-OH)} + A^\bullet$$

$$\text{Compound-I(HRP-Fe-OH)} + \text{AH} \rightarrow \text{HRP} + H_2O + A^\bullet$$

$$nA^\bullet \rightarrow A_n$$

where AH and A_n correspond to hydrogen donor (phenolic compound in this case) and the resulting polymer, respectively. When the hydrogen donor compound is guaiacol, the colored product of the reaction appears at 470 nm. As Fig. 6 inset indicates, catalysis of the same reaction by Fe(III)PPIX/MCM41 catalyst produces the same product at 470 nm, which means the catalyst mimicks peroxidase. Compare with peroxidase, the details of the process can be shown as follows (Scheme I):

In the presence of high concentrations of H_2O_2 (>3 mM), an irreversible inactivation process, namely "suicide inactivation process" can also take place [74,75]. During such inactivation hydrogen peroxide damages the porphyrin ring in C_I and converts it to an inactive verdoporphyrin (C_i) [74–77]. Results showed peroxide inactivation of catalyst occurs at [H_2O_2] > 3 mM. To avoid such inactivation effects, experiments were carried out below this concentration. Using the steady-state approximation for the active catalyst (C_I) gives:

$$\frac{dC_I}{dt} = k_1[H_2O_2][\text{Fe(III)PPIX}] - 2k_3[\text{AH}][C_I] - k_i[H_2O_2][C_I] = 0 \quad (1)$$

At low concentrations of hydrogen peroxide ([H_2O_2] < 3 mM), suicide inactivation reaction is negligible. Moreover, k_i (inactivation rate constant) is very small

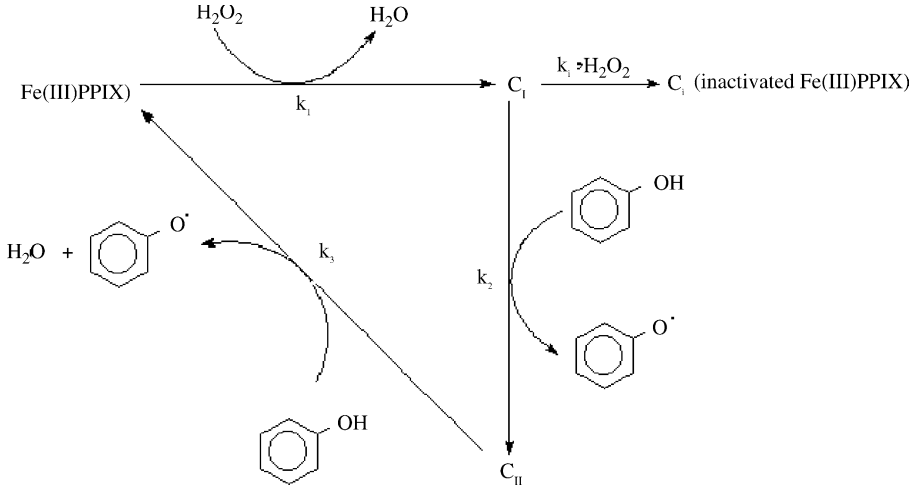

Scheme I.

($k_i \ll k_1$) and inactivation process is very slow. Hence, the above relation may be simplified as shown below:

$$\frac{dC_I}{dt} = k_1[H_2O_2][\text{Fe(III)PPIX}] - 2k_2[AH][C_I] = 0 \quad (2)$$

Thus, the $\mathbf{C_I}$ concentration can be written as a function of free Fe(III)PPIX concentration.

$$[C_I] = \frac{k_1[H_2O_2][\text{Fe(III)PPIX}]}{2k_2[AH]} \quad (3)$$

Using mass balance relations for [Fe(III)PPIX] and hydrogen peroxide, the rate of consumption of H_2O_2 could be obtained. This is useful in reactor design, scaling up the process and optimization of reaction conditions for industrial purposes, such as wastewater treatment (phenol removal process) [78,79]. Using the peroxidase enzyme model, the overall rate of consumption of H_2O_2 can be written as: [80,81]

$$\text{Rate} = \frac{d[H_2O_2]}{dt} = \frac{[\text{Fe(III)PPIX}]}{\frac{1}{k_1[H_2O_2]_0} + \frac{1}{k_3[AH]_0}} \quad (4)$$

At higher initial concentrations of AH ($[AH]_0$), the above equation can be simplified as:

$$k_3[AH_0] << k_1[H_2O_2]_0;\ \text{rate} = k_1[H_2O_2]_0 \cdot [\text{Fe(III)PPIX}] \quad (5)$$

k_1 rate constant could be obtained from the slope of the plot of rate of reaction versus catalyst concentration:

$$\text{Slope} = k_1[H_2O_2]_0$$

Fig. 7a shows such a plot for oxidation of guaiacol by hydrogen peroxide ($[H_2O_2]_0 = 2.0$ mM) from which k_1 is estimated equal to $9.595 \times 10^2\ M^{-1}\ s^{-1}$.

In a similar manner and at higher initial concentrations of guaiacol ($[AH]_0$), we have:

$$k_1[H_2O_2]_0 << k_3[AH_0];\ \text{rate} = k_3[AH]_0 \cdot [\text{Fe(III)PPIX}] \quad (6)$$

k_3 rate constant could be estimated from the slope of the linear plot of rate versus catalyst concentration:

$$\text{Slope} = k_3[AH]_0$$

Fig. 7b shows this plot for oxidation of guaiacol by hydrogen peroxide ($[AH]_0 = 2.8$ mM) from which k_3 is estimated equal to $1.029 \times 10^2\ M^{-1}\ s^{-1}$. Comparison of these k values with those of HRP, illustrates the reasonable catalytic activity of the enzyme model catalyst [Fe(III)PPIX]/MCM41 (see Table 2).

Also, by performing experiments (similar to that indicated in Fig. 6) at various guaiacol concentrations, it is possible to obtain the relevant Michaelis constant (K_m) for this enzyme model [82]. The method used for calculation of K_m and the other catalytic parameters are described below.

Peroxidase enzyme has a K_m value of about 1.5 μM for oxidation of phenolic compounds, such as guaiacol or

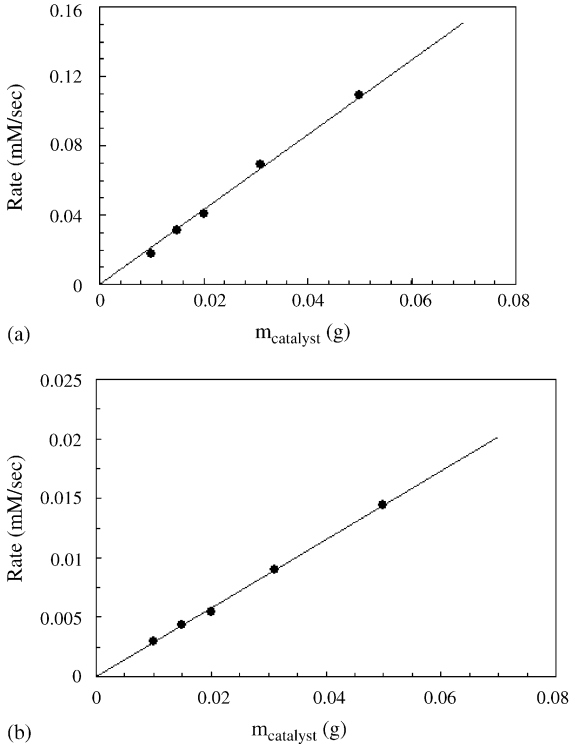

Fig. 7. Linear plots based on Eqs. (5) and (6) (as the rate vs. the amount of Fe(III)PPIX/MCM41 catalyst) for estimation of k_1 and k_3 rate constants. (a) Slope = $k_1 \times [H_2O_2]_0$, slope = 2.160, $[H_2O_2]_0 = 0.0020$ mM and (b) slope = $k_3 \times [AH]_0 \Rightarrow$ slope = 0.288, $[AH]_0 = 0.0028$ mM.

ABTS (2,2-azino-di-3-ethyl-benzothiazoline-(6)-sulphonic acid (ABTS) [83]. In the Michaelis–Menten model initial rates of reactions (υ_i) are plotted against the substrate concentration (guaiacol) based on a hyperbolic relation as follow:

$$V = \frac{V_{max}[S]}{([S] + K_m)} \quad (7)$$

In order to have a linear relation Lineweaver–Burk equation could be written as:

$$\frac{1}{V} = \frac{K_m}{V_{max}}\frac{1}{[S]} + \frac{1}{V_{max}} \quad (8)$$

The Lineweaver–Burk plot has been criticized on several grounds. Firstly, most impossible extrapolation across the $1/V$ axis to determine the value of $-1/K_m$. Secondly, it is said to give undue weight to measurements made at low substrate concentration. Thirdly, departures from linearity are less obvious than in some other plots, particularly the Eadie–Hofstee plot. Hence, in order to reach a reliable estimation of V_{max} and K_m, turnover number and catalytic efficiency it is better to use the Eadie–Hofstee plot as:

$$V = -K_m \times \left(\frac{V}{[S]}\right) + V_{max} \quad (9)$$

Fig. 8 shows such a plot for the Fe(III)PPIX/MCM41 system with $K_m = 183.1$ μM and $V_{max} = 0.171$ mM s^{-1}. Although the obtained K_m value is large in relation to the peroxidase K_m, it

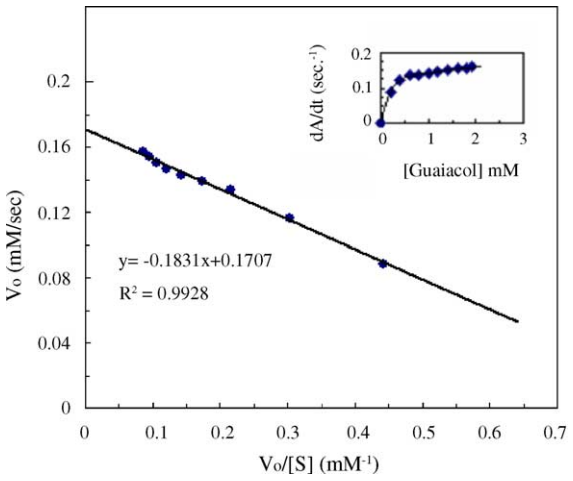

Fig. 8. Eadie–Hofstee plot according to Eq. (9) for oxidation of guaiacol by Fe(III)PPIX/MCM41 catalyst $[H_2O_2] = 2.0$ mM and Fe(III)PPIX/MCM41 = 0.010 g.

indicates potential for application of Fe(III)PPIX/MCM41 catalyst for industrial purposes. Some citable processes include phenol removal from aqueous solutions, oxidation/polymerization of aromatic hydrogen donors (preparation of conductive polymers), epoxidation of alkenes and hydroxylation reactions. It must be mentioned that there are various limitations for using peroxidase in such industrial processes.

Turnover number or catalytic rate constant (k_{cat}) which represents the maximum number of moles of substrate converted to the product per number of moles of catalyst per unit time, could be obtained from $k_{cat} = V_{max}/[catalyst]$. The value of turnover number was obtained equal to 1.71×10^4 (moles of guaiacol/moles of Fe(III)PPIX per second) as obtained from data of Fig. 8. Also catalytic efficiency of the synthetic model enzyme catalyst, which is defined as k_{cat}/K_m was calculated to be 9.3443×10^4. This finding shows Fe(III)PPIX/MCM41 could be used as a peroxidase mimicking catalyst, indicating that it could be introduced as an industrial alternative for the peroxidase enzyme. Fig. 9 shows the capability of the catalyst for synthesis of indophenol from phenol and aniline. The reaction is followed spectrophotometrically at 630 nm. The experimental conditions were [aniline] = 10.0 mM, [phenol] = 2.0 mM, $[H_2O_2] = 2.0$ mM and Fe(III)PPIX/MCM41 = 0.010 g. The synthesis reaction was completed within 40 min. Table 1 shows and compares the capability of Fe(III)PPIX/MCM41 toward various peroxidatic reactions including phenol oxidation, guaiacol oxidation and indophenol synthesis in the presence of hydrogen peroxide. As the table indicates, for all the tests, blank experiments were carried out using Fe(III)/MCM41 catalyst. According to Table 1, in the most cases no detectable reaction was observed in the presence of Fe(III)/MCM41. This fact reflects the important role of porphyrin group in Fe(III)PPIX that provides higher oxidation states for iron and subsequent generation of highly oxidant species (C_I and C_{II} in Scheme I).

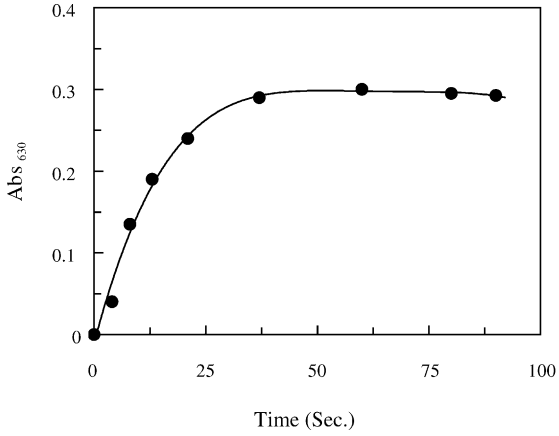

Fig. 9. Typical progress curve for synthesis of indophenol by Fe(III)PPIX/MCM41 catalyst, [aniline] = 10.0 mM, [phenol] = 2.0 mM, $[H_2O_2] = 2.0$ mM and Fe(III)PPIX/MCM41 = 0.020 g.

Table 1
Catalytic (peroxidatic) activities of Fe(III)PPIX/MCM41 catalyst for various oxidation reactions

Catalyst	Reaction	Initial rate (mM min^{-1})
Fe(III)PPIX/MCM41	Indophenol synthesis	0.01120
Fe(III)PPIX/MCM41	Phenol oxidation	0.01545
Fe(III)PPIX/MCM41	Guaiacol oxidation	0.02122
Fe(III)/MCM41	Guaiacol oxidation	0.00027
Fe(III)/MCM41	Phenol oxidation	No reaction
Fe(III)/MCM41	Indophenol synthesis	No reaction

Control reactions were carried out using Fe(III)/MCM41 as the blank catalyst.

Table 2 shows the relative k values for HRP, Fe(III)PPIX/MCM41 and Fe(III)/MCM41. Comparison of k_1 for Fe(III)PPIX/MCM41 and HRP shows some meaningful and considerable differences between their catalytic activities, which may arise from the structure and high specificity of the enzyme for such substrates and reactions. However, rate constants for the enzyme model catalyst Fe(III)PPIX/MCM41 are sufficiently large to complete such reactions in longer periods of time. There are several limitations for the use of peroxidase in severe industrial conditions. Generally, enzyme structure denatures at high temperatures and pressures, in highly acidic or alkaline media, organic solvents and denaturants. In most cases, such a denaturation is associated with deactivation of the enzyme.

Considering these limitations, inorganic heterogeneous catalysts, which can mimic the peroxidase reactions, could be introduced as suitable candidates for industrial purposes.

Table 2
Comparative rate constants values for HRP, Fe(III)PPIX/MCM41, and Fe(III)/MCM41 catalysts

Catalyst	k_1 (M^{-1} s^{-1})	k_3 (M^{-1} s^{-1})
Horseradish peroxidase	$1.42 \times 10^7 \pm 2 \times 10^5$	$1.30 \times 10^5 \pm 2.6 \times 10^3$
Fe(III)PPIX/MCM41	$9.595 \times 10^2 \pm 25$	$1.029 \times 10^2 \pm 3.21$
Fe(III)/MCM41	$8.858 \times 10^1 \pm 3.12$	7.876 ± 0.385

Acknowledgements

The financial supports of the Research Council of Islamic Azad University, Research Council of the University of Tehran and Iran National Science Foundation are gratefully acknowledged.

References

[1] H. Hatzikonstantinou, S.B. Brown, Biochem. J. 174 (1978) 893–900.
[2] P. Jones, D. Mantle, I. Wilson, J. Chem. Soc., Dalton Trans. (1983) 161–164.
[3] P. Jones, T. Bobson, S.B. Brown, Biochem. J. 135 (1973) 353–359.
[4] N. Kamiya, S. Furusaki, M. Goto, Biotechnol. Lett. 19 (1997) 1115–1118.
[5] M. Momenteau, Biochim. Biophys. Acta 304 (1973) 814–827.
[6] R.W. Hay, Bio-Inorganic Chemistry, Ellis Harwood Limited, New York, 1991.
[7] G. Palmer, in: D. Dolphin (Ed.), The Porphyrins, Academic Press, New York, 1978.
[8] D. Portsmouth, E.A. Beal, Eur. J. Biochem. 19 (1971) 479–487.
[9] N. Kamiya, M. Goto, S. Furusaki, Biotechnol. Bioeng. 64 (4) (1999) 502–506.
[10] B.T. Holland, C. Walkup, A. Stein, J. Phys. Chem. B 102 (1998) 4301–4309.
[11] I.V. Kozhevnikov, A. Sinnema, R.J.J. Jansen, K. Pamin, H. van Bekkum, Catal. Lett. 30 (1–2) (1995) 241–252.
[12] E. Armengol, M.L. Cano, H. Garcia, M.T. Navarro, J. Chem. Soc. Chem. Commun. (1995) 519–520.
[13] R.K. Kloetstra, H. van Bekkum, J. Chem. Res. (Symp.) (1995) 26–27.
[14] R.K. Kloetstra, H. van Bekkum, J. Chem. Soc. Chem. Commun. (1995) 1005–1006.
[15] X.S. Zhao, G.Q. Lu, G.J. Millar, Ind. Eng. Chem. Res. (1996) 2075–2090.
[16] J.S. Beck, C. Vartuli, W.J. Roth, M.E. Leonowicz, C.T. Kresge, K.D. Schmitt, C.T.W. Chu, D.H. Olson, E.W. Sheppard, S.B. McCullen, J.B. Higgins, J.L. Schlenker, J. Am. Chem. Soc. 114 (1992) 10834–10843.
[17] C.T. Kresge, M.E. Leonowicz, W.J. Roth, J.C. Vartuli, J.S. Beck, Nature 359 (1992) 710–712.
[18] J.S. Beck, R.F. Socha, D.S. Shihabi, J.C. Vartuli, US Patent 5,143,707 (1992).
[19] J.S. Beck, J.C. Vartuli, G.J. Kennedy, C.T. Kresge, W.J. Roth, S.E. Schramm, Chem. Mater. 6 (1994) 1816–1821.
[20] A. Sayari, C. Danumah, I.L. Moudrakovski, Mater. Res. Soc. Symp. Proc. 371 (1995) 81–92.
[21] J. Chen, Q. Li, R. Xu, F. Xiao, Angew. Chem. Int. Ed. Engl. 34 (1995) 2694–2701.
[22] M. Alvaro, H. Garcia, S. Garcia, F. Marquez, J.C. Scaino, J. Phys. Chem. B 101 (1997) 3043–3051.
[23] L. Mercier, T.J. Pinnavaia, Adv. Mater. 9 (1997) 500–507.
[24] X. Fang, G.E. Fryxell, L.Q. Wang, A.Y. Kim, J. Liu, K.M. Kemner, Science 276 (1997) 923–926.
[25] J. Liu, X. Feng, G.E. Fryxell, L.Q. Wang, A.Y. Kim, M. Gong, Adv. Mater. 10 (1998) 161–168.
[26] A. Cauvel, G. Renard, D. Brunel, J. Org. Chem. 62 (1997) 749–756.
[27] P. Sutra, D. Brunel, Chem. Commun. (1996) 2485–2488.
[28] Y.V. Subba Rao, D.E. Devos, T. Bein, P.A. Jacobs, Chem. Commun. (1997) 355–358.
[29] Y.V. Subba Rao, D.E. Devos, P.A. Jacobs, Angew. Chem. Int. Ed. Engl. 36 (1997) 2661–2669.
[30] S. O'Brien, J. Tudor, S. Barlow, M.J. Drewitt, S.J. Heyes, D. O'Hare, Chem. Commun. (1997) 641–644.
[31] W. Bohlmann, K. Schandert, A. Poppl, H.C. Semmelhack, Zeolites 19 (1997) 297–303.
[32] L. Frunza, H. Landmesser, E. Haft, R. Fricke, J. Mol. Catal. A 123 (1997) 179–186.
[33] G. Britovsek, J. Chem. Commun. (1998) 849–850.
[34] R. Hoppe, A. Ortlam, J. Rathousky, G.Z. Schulz-Ekloff, A. Zukal, Microporous Mater. 8 (1997) 267.
[35] Ch. Liu, Y. Shan, X. Yang, X. Ye, Y. Wu., J. Catal. 168 (1997) 35–41.
[36] S.S. Kim, W. Zhang, T. Pinnavaia, J. Catal. Lett. 43 (1997) 149.
[37] Y.J. Ying, L. Zhang, T. Sun, US Patent 6,028,025 (2000).
[38] Z. Wuzong, Science 280 (1998) 5364.
[39] C.J. Liu, Sh. G. Li, W. Qinpang, Ch. M. Che, J. Chem. Commun. (1997) 65–66.
[40] X.S. Zhao, G.Q. Lu, G.J. Millar, X.S. Li, Catal. Lett. 38 (1996) 33–36.
[41] C.Y. Chen, H.Y. Li, M.E. Davis, Microporous Mater. 2 (1993) 17–26.
[42] C.Y. Chen, H.Y. Li, M.E. Davis, Microporous Mater. 2 (1993) 27–34.
[43] J.C. Vartuli, K.D. Schmitt, C.T. Kresge, W.J. Roth, M.E. Leonowicz, S.B. McCullen, S.D. Hellring, J.S. Beck, J.L. Schlenker, D.H. Olson, E.W. Sheppard, Chem. Mater. 6 (1994) 2317–2326.
[44] S.P. Naik, A.S.T. Chiang, R.W. Thompson, F.C. Huang, H.M. Kao, Microporous Mesoporous Mater. 60 (2003) 213–224.
[45] R. Tismaneanu, B. Ray, R. Khalfin, R. Semiat, M.S. Eisen, J. Mol. Catal. A 171 (2001) 229–241.
[46] F. Di Renzo, H. Cambon, R. Dutartre, Microporous Mater. 10 (1997) 283–286.
[47] W.J. Kim, Y.J. Churl, D.T. Hayhurst, Microporous Mesoporous Mater. 49 (2001) 125–137.
[48] C. Berlini, G. Ferraris, M. Guidotti, G. Moretti, R. Psaro, Microporous Mesoporous Mater. 44 (2001) 595–602.
[49] M.O. Coppens, J. Sun, T. Maschmeyer, Catal. Today 69 (1) (2001) 331–335.
[50] U. Oberhagemann, M. Jeschke, H. Papp, Microporous Mesoporous Mater. 33 (1999) 165–172.
[51] J. Yu, J.L. Shi, L.Z. Wang, M.L. Ruan, D.S. Yan, Ceram. Int. 26 (2000) 359–362.
[52] J. Rathousky, A. Zukai, O. Franke, G. Schulz-Ekloff, J. Chem. Soc., Faraday Trans. 90 (1994) 2821–2826.
[53] J. Rathousky, A. Zukai, O. Franke, G. Schulz-Ekloff, J. Chem. Soc., Faraday Trans. 91 (1995) 937–940.
[54] R. Schmidt, E.W. Hansen, M. Stocker, D. Akpriaye, O.H. Ellestad, J. Am. Chem. Soc. 117 (1995) 4049–4056.
[55] J.C. Vartuli, A. Malek, W.J. Roth, C.T. Kresge, S.B. McCullen, Microporous Mesoporous Mater. 44 (2001) 691–695.
[56] A.B. Bourlinos, M.A. Karakassides, D. Petridis, J. Phys. Chem. B 104 (1999) 4375–4380.
[57] A.C. Maehly, B. Chance, in: S.P. Colowick, N.O. Kaplan (Eds.), Methods Enzymol, vol. 2, Academic Press, New York, 1965, pp. 764–775.
[58] P. George, Biochem. J. 54 (1953) 267–271.
[59] X.S. Zhao, G.Q. Lu, A.K. Whittaker, G.J. Millar, H.Y. Zhu, J. Phys. Chem. B 101 (1997) 6525–6531.
[60] L. Nikiel, T.W. Zerda, J. Phys. Chem. 95 (1991) 4063–4071.
[61] G. Behrens, G.D. Stucky, Angew. Chem. Int. Ed. Engl. 32 (1993) 666–669.
[62] C.Y. Chen, H.X. Li, M.E. Davis, Microporous Mater. 2 (1993) 17–26.
[63] H.Y. Zhu, X.S. Zhao, G.Q. Lu, D.D. Do, Langmuir 12 (1996) 6513–6517.
[64] S.J. Cregg, K.S.W. Sing, Adsorption Surface Area and Porosity, second ed., Academic Press, New York, 1982.
[65] P.J. Branton, K.S.W. Sing, J. Chem. Soc. Chem. Commun. (1993) 1257–1258.
[66] M.M.L. Ribeiro Carrott, A.J.E. Candeias, P.J.M. Carrott, P.I. Ravikovitch, A.V. Neimark, A.D. Sequeira, Microporous Mesoporous Mater. 47 (2001) 323–337.

[67] B.T. Holland, Ch. Walkup, A. Stein, J. Phys. Chem. B 102 (1998) 4301–4309.
[68] M. Stockenhubev, M.J. Hudson, W.R. Joyner, J. Phys. Chem. B 104 (2000) 3370–3374.
[69] A.B. Bourlinos, M.A. Karakassides, D. Petridis, J. Phys. Chem. B 104 (2000) 4375–4380.
[70] F. Algarra, M.A. Esteves, V. Fornes, H. Garcia, J. Primoj, New J. Chem. 22 (4) (1998) 333–338.
[71] D.L. Pavia, G.M. Lampman, G.S. Kriz, Introduction to Spectroscopy (1987) 49, Chapter 1.
[72] The Aldrich Library of Infrared Spectra, third ed., 1992.
[73] H.B. Dunford, Heme Peroxidases, John Wiley & Sons, New York, 1999.
[74] K.J. Baynton, J.K. Bewtra, N. Biswas, K.E. Taylor, Biochim. Biophys. Acta 1206 (1993) 272–278.
[75] A.N.P. Hiner, J. Hernandez-Ruiz, M.B. Arnao, F. Garcia-Canovas, M. Acosta, Biotechnol. Bioeng. 50 (1996) 655–662.
[76] A.A. Moosavi-Movahedi, K. Nazari, M. Ghadermarzi, Ital. J. BIOC. 48 (1) (1999) 9–17.
[77] K. Nazari, A. Mahmoudi, M. Shahrooz, A.A. Moosavi-Movahedi, J. Enzyme Inhib. Med. Chem., in press.
[78] M. Masuda, A. Sakurai, M. Sakakibara, Enzyme Microb. Technol. 28 (2001) 295–300.
[79] I.D. Buchannan, J.A. Nicell, J. Chem. Technol. Biotechnol. 72 (1998) 23–32.
[80] A.C. Maehly, Methods Enzymol. 2 (1972) 801–813.
[81] B. Farzami, K. Nazari, A.A. Moosavi-Movahedi, J. Sci. I.R. Iran 8 (1997) 209–216.
[82] T. Palmer, Understanding Enzymes, third ed., Ellis Harwood Publication, Sussex, 1991, pp. 118–125.
[83] N. Kumar, D.R. Tripathi, Plant Peroxidase Newsletter 15 (1999) 45–48.